VOLUME 11 NUMBER 9 SEPTEMBER 2009 www.cell-micro.com ISSN 1462-5814

cellular microbiology

Thematic Reviews: Innate Defenses

Hepatitis E virus

Plasmodium berghei parasites

WILEY-BLACKWELL

Cover Image. Human HEK-293 cells (blue nuclei) were transfected with shRNAs causing knockdown of RABEP1 resulting in increased vacuolar escape of listeriolysin-deficient *Listeria monocytogenes*. This image shows large numbers of cytosolic *L. monocytogenes* (green) associated with host cell F-actin (red).

See article by Burrack et al., Perturbation of vacuolar maturation promotes listeriolysin O-independent vacuolar escape during *Listeria monocytogenes* infection of human cells, pgs. 1382-1398.

Cellular Microbiology (2009) **11**(9), 1382–1398
doi:10.1111/j.1462-5822.2009.01338.x
First published online 23 June 2009

Perturbation of vacuolar maturation promotes listeriolysin O-independent vacuolar escape during *Listeria monocytogenes* infection of human cells

Laura S. Burrack,[1†] J. Wade Harper[2] and Darren E. Higgins[1*]
[1]*Department of Microbiology and Molecular Genetics, Harvard Medical School, 200 Longwood Avenue, Boston, MA 02115, USA.*
[2]*Department of Pathology, Harvard Medical School, 77 Avenue Louis Pasteur, Boston, MA 02115, USA.*

Summary

Listeria monocytogenes **is a bacterial pathogen that replicates within the cytosol of infected host cells. The ability to rapidly escape the phagocytic vacuole is essential for efficient intracellular replication. In the murine model of infection, the pore-forming cytolysin listeriolysin O (LLO) is absolutely required for vacuolar dissolution, as LLO-deficient (ΔLLO) mutants remain trapped within vacuoles. In contrast, in many human cell types ΔLLO *L. monocytogenes* are capable of vacuolar escape at moderate to high frequencies. To better characterize the mechanism of LLO-independent vacuolar escape in human cells, we conducted an RNA interference screen to identify vesicular trafficking factors that play a role in altering vacuolar escape efficiency of ΔLLO *L. monocytogenes*. RNA interference knockdown of 18 vesicular trafficking factors resulted in increased LLO-independent vacuolar escape. Our results suggest that knockdown of one factor, RABEP1 (rabaptin-5), decreased the maturation of vacuoles containing ΔLLO *L. monocytogenes*. Thus, we provide evidence that increased vacuolar escape of ΔLLO *L. monocytogenes* in human cells correlates with slower vacuolar maturation. We also determined that increased LLO-independent dissolution of vacuoles during RABEP1 knockdown required the bacterial broad-range phospholipase C (PC-PLC). We hypothesize that slowing the kinetics of vacuolar maturation generates an environment conducive for vacuolar escape mediated by the bacterial phospholipases.**

Received 7 April, 2009; revised 20 May, 2009; accepted 23 May, 2009. *For correspondence. E-mail dhiggins@hms.harvard.edu; Tel. (+1) 617 432 4156; Fax (+1) 617 738 7664.
†Present address: Department of Genetics, Cell Biology, and Development, University of Minnesota, 420 Washington Avenue SE, Minneapolis, MN 55455, USA.

Introduction

Listeria monocytogenes is a facultative intracellular bacterial pathogen capable of infecting a wide variety of species. Upon entry into host cells, *L. monocytogenes* escapes the entry vacuole, replicates within the cytosol and uses actin-based motility to spread to neighbouring cells resulting in formation of secondary double-membrane vacuoles. Once in neighbouring cells, *L. monocytogenes* escapes the secondary vacuole and begins replicating again in the cytosol (Tilney and Portnoy, 1989). Vacuolar dissolution is essential for intracellular growth as *L. monocytogenes* fails to replicate or replicates inefficiently within vacuoles (Portnoy *et al.*, 1988; Cheng and Portnoy, 2003; Birmingham *et al.*, 2008). In all murine cells examined, the bacterial pore-forming cytolysin listeriolysin O (LLO, encoded by *hly*) is absolutely required for vacuolar escape. Consistent with vacuolar escape being essential for intracellular growth, LLO-deficient *L. monocytogenes* strains (ΔLLO) are avirulent in the murine infection model (Portnoy *et al.*, 1988). Based on these results, inhibitors of LLO have been proposed as alternative or supplemental treatments for *L. monocytogenes* infections (Edelson and Unanue, 2001).

However, in contrast to what is observed in the murine system, some human epithelial cells, such as HeLa and HEp-2 cells, permit efficient vacuolar escape of ΔLLO *L. monocytogenes* (Grundling *et al.*, 2003). Additionally, primary human dendritic cells and human WS-1 skin fibroblasts have been previously shown to allow vacuolar escape of ΔLLO *L. monocytogenes*, but at much lower levels than wild-type bacteria (Portnoy *et al.*, 1988; Paschen *et al.*, 2000). Similar results have been observed recently in our lab for a number of other human cell lines including HepG2 (hepatocytes), Hct116 (colon epithelial cells) and HEK-293 (kidney epithelial cells) (L.S. Burrack

and D.E. Higgins, unpublished). These results suggest that inhibitors of LLO may be an effective treatment for *L. monocytogenes* infections in the murine infection model, but not in humans. Therefore, we sought to better understand the role of LLO and additional bacterial/host cell factors mediating efficient vacuolar escape in human cells.

The observation that some human cells are permissive for vacuolar escape of ΔLLO *L. monocytogenes* was first made over 20 years ago (Portnoy *et al*., 1988), but the differences in the vacuolar biology of human cells that allow LLO-independent vacuolar escape have not been described. In human cell lines permissive for vacuolar escape of ΔLLO *L. monocytogenes*, the bacterial broad-range phospholipase C (PC-PLC) was shown to be essential for vacuolar escape (Marquis *et al*., 1995; Grundling *et al*., 2003; Alberti-Segui *et al*., 2007). *L. monocytogenes* also encodes a phosphatidylinositol-specific phospholipase, PI-PLC (Camilli *et al*., 1993). PI-PLC assists LLO and PC-PLC in lysis of primary vacuoles and secondary double-membrane vacuoles (Smith *et al*., 1995). The bacterial phospholipases appear to work synergistically during infection as deletion of both phospholipases results in a more severe defect in vacuolar dissolution than would be expected from the phenotypes observed following deletion of either phospholipase alone (Smith *et al*., 1995).

LLO is a member of the cholesterol-dependent cytolysin family and has optimum pore-forming activity at an acidic pH (Beauregard *et al*., 1997). The pH dependence of the pore-forming activity of LLO is important for compartmentalizing the activity of the protein to the vacuole and thus preventing cytotoxicity by LLO secreted from bacteria replicating in the cytosol (Glomski *et al*., 2002). However, the requirement of an acidic pH environment for proper function of LLO makes *L. monocytogenes* dependent on partial maturation of the vacuole to facilitate efficient lysis of the vacuole. Treatment of murine macrophages with bafilomycin A1, an inhibitor of vacuolar ATPase activity, or knockdown of vacuolar ATPase subunits by RNA interference (RNAi) in *Drosophila* hemocytes results in vacuoles that do not acidify and inefficient vacuolar escape by *L. monocytogenes* (Beauregard *et al*., 1997; Agaisse *et al*., 2005). In murine macrophages, *L. monocytogenes* is thought to efficiently escape from RAB7-positive compartments resembling late endosomes. However, the ability of bacteria to escape from mature vacuoles containing lysosomal-associated membrane protein 1 (LAMP1) has been shown to be much less efficient than from RAB7-positive late endosome-like vacuoles (Henry *et al*., 2006). This result suggests that maturation beyond a late endosome-like compartment is detrimental for vacuolar dissolution by *L. monocytogenes*.

Recent studies demonstrate that LLO activity affects vacuolar maturation during infection. Swanson and colleagues have shown that in murine RAW 264.7 cells, vacuoles containing wild-type *L. monocytogenes* exhibit slower maturation than vacuoles containing ΔLLO bacteria (Henry *et al*., 2006). Furthermore, it was shown that LLO causes small perforations in the vacuolar membrane prior to bacterial escape causing uncoupling of pH and calcium gradients (Shaughnessy *et al*., 2006). Based on these observations, we hypothesized that one of the functions of LLO during infection is to slow vacuolar maturation and that alterations in vacuolar maturation kinetics in some human cell lines provides a more conducive environment for PC-PLC to mediate vacuolar escape of *L. monocytogenes* in the absence of LLO activity.

Our group and others have previously used RNAi as a method to identify host factors required for intracellular bacterial infection. RNAi in *Drosophila* tissue culture cells has been used to identify host factors required for infection by *L. monocytogenes*, *Mycobacterium fortuitum*, *Legionella pneumophila* and *Chlamydia caviae* (Agaisse *et al*., 2005; Cheng *et al*., 2005; Philips *et al*., 2005; Dorer *et al*., 2006; Derre *et al*., 2007). Additionally, Portnoy and co-workers used a combination of *L. monocytogenes* mutants with a genome-scale *Drosophila* RNAi screen to further characterize the interaction of bacterial virulence factors and host cells (Cheng *et al*., 2005). One of the bacterial strains used was ΔLLO *L. monocytogenes*. Their results indicated that RNAi knockdown of several members of the host multivesicular body (MVB) required for transition between late endosomes and lysosomes led to increased vacuolar escape of ΔLLO *L. monocytogenes* in *Drosophila* cells (Cheng *et al*., 2005). However, these results were not confirmed in human cells nor was the mechanism permitting increased vacuolar escape characterized. Compared with the *Drosophila* system, large-scale RNAi screens have been used to a much more limited extent in human cells for studies of interactions between bacterial pathogens and their hosts, as most research using RNAi techniques in mammalian cells has focused on knockdown of specific host cell proteins (Knodler *et al*., 2005; Ohya *et al*., 2005). Recently, Kuijl *et al*. (2007) used a subgenomic library of small interfering RNAs targeting the human kinome to identify kinases required for efficient intracellular infection of *Salmonella enterica* serovar Typhimurium and *Mycobacterium tuberculosis*.

In this work, we designed and completed an RNAi screen in human cells to identify vesicular trafficking host cell factors that play a role in altering vacuolar escape of ΔLLO *L. monocytogenes*. We provide evidence that shRNA treatments resulting in a significant increase in vacuolar escape by ΔLLO bacteria also slow

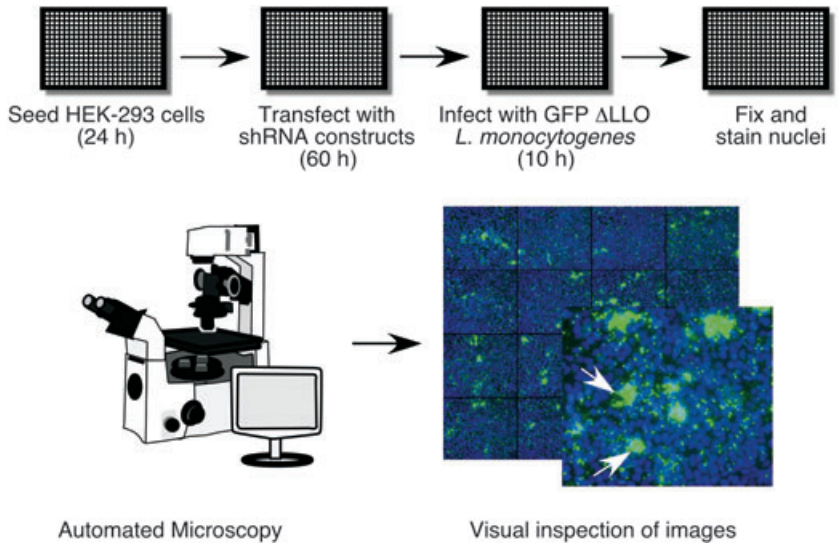

Fig. 1. Schematic of screen design to identify shRNAs targeting vesicular trafficking gene products that allow increased intracellular growth of ΔLLO *L. monocytogenes*. Following treatment with shRNAs, cells were infected with GFP-expressing ΔLLO *L. monocytogenes* at an moi of 5. One hour post infection, gentamicin was added to kill extracellular bacteria. At 10 h post infection, the cells were fixed and host nuclei were stained with Hoechst dye. Automated microscopy was used to obtain two images per well. The white arrows point to representative HEK-293 cells in which ΔLLO *L. monocytogenes* bacteria have escaped the vacuole and replicated efficiently.

the vacuolar maturation process. Our work supports a role for LLO in modulating vacuolar maturation in host cells and suggests that the ability of LLO to alter the vacuolar maturation process is indeed functionally important during *L. monocytogenes* infection of mammalian hosts.

Results

RNAi screen to identify host cell factors that facilitate LLO-independent vacuolar escape

To identify host cell vesicular trafficking components that play a role in preventing efficient vacuolar escape of ΔLLO *L. monocytogenes* in human cells, we first compiled a small hairpin RNA (shRNA) library containing 211 hairpins targeting 72 gene products with functional roles in vesicular trafficking (Table S1). The majority of the human homologues for the vesicular trafficking proteins identified in the genome-wide *Drosophila* RNAi screen performed in our lab (Agaisse *et al*., 2005) and a similar screen performed by Portnoy and co-workers (Cheng *et al*., 2005) were included along with other selected targets predicted to be in the same vesicular trafficking pathways. The subgenomic library was constructed by selecting individual shRNA clones from a previously constructed genome-wide pSMC2 shRNA library (Silva *et al*., 2005). The pSMC2 shRNAs were designed to more closely mimic naturally occurring microRNA transcripts. This design has been shown to produce shRNAs that are more potent than constructs that do not mimic microRNAs. The increased potency is likely due to better processing of the shRNA by Dicer into duplexes capable of interacting with RISC in a manner that results in efficient mRNA degradation (Silva *et al*., 2005).

We then used this library to screen for shRNAs targeting vesicular trafficking gene products that caused increased vacuolar escape of ΔLLO *L. monocytogenes* in human cells. For our screen, we used HEK-293 human kidney epithelial cells. HEK-293 cells are easily transfectable. Also, in untreated HEK-293 cells, a very low level of vacuolar escape (< 1%) of ΔLLO *L. monocytogenes* is observed. For the screen, HEK-293 cells were transfected with each shRNA in black, clear-bottom 96-well plates. A small amount of dsRed-encoding plasmid (1/10 total DNA amount) was co-transfected to estimate the transfection efficiency. Typically, greater than 90% of cells in each well were dsRed-positive. After incubating the transfected HEK-293 cells for 60 h to allow for RNAi-mediated knockdown of target gene products, transfected cells were infected with GFP-expressing ΔLLO *L. monocytogenes* for 10 h. Host cell nuclei were then stained with Hoechst dye to allow for the determination of the number of host cells per well. Intracellular growth of ΔLLO *L. monocytogenes* was monitored by automated fluorescence microscopy (Fig. 1). Replication of ΔLLO *L. monocytogenes* within membrane-bound vacuoles of HEK-293 cells is inefficient. Therefore, high levels of bacteria within host cells indicate that *L. monocytogenes* has escaped the vacuole and has replicated efficiently in the cytosol. We tested this assumption by staining infected cells with Texas Red-phalloidin. In host cells with large numbers, *L. monocytogenes* bacteria were stained with Texas Red-phalloidin indicating association with host cell F-actin, an established marker of *L. monocytogenes* vacuolar escape. To estimate vacuolar escape, we counted the number of cells in each image that were filled with bacteria (escape events) as shown by white arrows in Fig. 1. Escape events were quantified in

two images per well and the screen was performed in duplicate (four images/shRNA in total). For untreated HEK-293 cells, the mean number of escape events observed was 1.8 ± 0.8 per image. If the mean number of escape events in shRNA-transfected wells was greater than two standard deviations above the mean number of escape events observed in untreated cells (> 3.4 events per image), the shRNA treatment was determined to increase vacuolar escape.

We identified 32 hairpins targeting 18 gene products that increased vacuolar escape of ΔLLO *L. monocytogenes* (Table 1). All hairpins identified were sequenced to ensure that the inserts were correct and that the shRNA targeted the intended gene product. We chose 10 gene products for further analysis (ARCN1, COPG, EEA1, RAB21, RAB4A, RAB5C, RABEP1, SEC15L1, CTSL and VPS28). Because the pBlueScript-based vector pBS-mir is a more stable vector for repeated propagation in *Escherichia coli* than pSMC2 (Li and Elledge, 2005; Silva *et al*., 2005), the shRNA inserts targeting the selected gene products were transferred from the pSMC2 vesicular trafficking library plasmids to pBS-mir. Each shRNA insert that was successfully transferred to a pBS-mir vector was then analysed and the vacuolar escape frequency of ΔLLO *L. monocytogenes* was quantified by determining the mean number of escape events in four images per well in three separate experiments. Control shRNAs targeting GFP and firefly luciferase were also included in these experiments. The mean number of escape events per image for all experiments performed with each shRNA insert is indicated in Table 1.

In untreated wells and wells transfected with GFP and firefly luciferase control shRNAs, escape events occurred in approximately 1% of HEK-293 cells. Among all of the shRNA treatments examined, knockdown of several COP-I coatomer subunits and RABEP1 resulted in the highest levels of vacuolar escape of ΔLLO *L. monocytogenes* with vacuolar escape events occurring in approximately 5–10% of HEK-293 cells. Based on these results and our interest in the effect of alterations in early stages of vacuolar maturation on *L. monocytogenes* infection, we decided to further characterize the role of RABEP1 in modulating vacuolar escape of ΔLLO *L. monocytogenes*. RABEP1 is an effector of RAB5A and RAB4A (Pagano *et al*., 2004) and functions in early endosome and recycling endosome formation. RAB4A was also identified in the RNAi screen. Several other gene products with roles in early endosomes and endosome recycling were also identified (Table 1). The significant increase in escape events observed following knockdown of RABEP1 might occur because RABEP1 functions in the regulation of both the early endosome and recycling endosome pathways.

Knockdown of RABEP1 correlates with increased LLO-independent vacuolar escape

Three shRNAs targeting RABEP1 were in the vesicular trafficking subgenomic library (Table S1). Two of these hairpins, v2HS_37113 and v2HS_37115 (RABEP1-1 and RABEP1-3 respectively), resulted in an increased frequency of HEK-293 cells in which efficient growth of ΔLLO *L. monocytogenes* was observed (Table 1). To further demonstrate that knockdown of RABEP1 resulted in increased vacuolar escape, we performed Western blots and infection experiments in parallel with shRNA-transfected HEK-293 cells. Depletion of RABEP1 protein was observed upon treatment with the RABEP1-1 and RABEP1-3 hairpins (Fig. 2A), which also resulted in increased vacuolar escape (Fig. 2B). Knockdown of RABEP1 was most efficient following transfection of the RABEP1-1 shRNA. However, transfection of the RABEP1-2 hairpin (v2HS_37116) failed to decrease RABEP1 protein levels or alter vacuolar escape of ΔLLO *L. monocytogenes* (Fig. 2A and B). To further show that ΔLLO bacteria in highly infected host cells were located within the cytosol, we infected shRNA-transfected HEK-293 cells with GFP-expressing ΔLLO bacteria and then stained host cell actin with Texas Red-phalloidin. *L. monocytogenes* in highly infected cells transfected with the RABEP1-1 and RABEP1-3 hairpins were associated with cytosolic host cell F-actin indicating that bacteria had escaped the vacuole (Fig. 2C).

Knockdown of RABEP1 increases LLO-independent vacuolar escape in Hct116 cells

To ensure that the results we observed were not specific to HEK-293 cells, we determined the efficiency of vacuolar escape in Hct116 human colon epithelial cells following knockdown of vesicular trafficking gene products identified in the RNAi screen. We transfected Hct116 human epithelial colon cells with shRNAs targeting COPG, CTSL and RABEP1. These gene products were chosen because they represent three distinct functional categories of vesicular trafficking gene products identified (Table 1). As untreated Hct116 cells are more permissive for vacuolar escape of ΔLLO *L. monocytogenes* than HEK-293 cells, the increase in vacuolar escape observed for shRNA-treated Hct116 cells was less dramatic than that in HEK-293 cells. However, similar results were observed in both human-derived cell lines, as knockdown of COPG, CTSL and RABEP1 (data not shown and Fig. 3) significantly increased vacuolar escape and intracellular replication of ΔLLO *L. monocytogenes* in both HEK-293 cells (Fig. 3A and B) and Hct116 cells (Fig. 3C and D), indicating that the results are likely applicable to multiple human-derived cell lines.

Table 1. Gene products targeted by shRNAs identified as causing increased bacterial growth of ΔLLO *L. monocytogenes*.

Gene	Full gene name	Accession #	Functional annotation	Hairpin ID	# images	# escaped/image
Golgi-related gene products						
ARCN1	Archain 1	NM_001655.3	Coatomer subunit	v2HS_132658*	16	11.2
				v2HS_132662*	16	8.6
ARF1	ADP-ribosylation factor 1	NM_001658.2	ADP-ribosylation	v2HS_132681	4	6.5
COPB	Coatomer protein complex, subunit beta	NM_016451.3	Coatomer subunit	v2HS_115883	4	11.8
COPG	Coatomer protein complex, subunit gamma	NM_016128.3	Coatomer subunit	v2HS_97705*	16	8.3
				v2HS_231877*	16	5.2
COPG2	Coatomer protein complex, subunit gamma 2	NM_012133.1	Coatomer subunit	v2HS_16398	4	14.8
RAB2A	RAB2, member RAS oncogene family	NM_002865.1	ER-Golgi	v2HS_171124	4	5.5
				v2HS_221483	4	6.0
				v2HS_219970	4	8.5
SARA2	SAR1a gene homologue 2	NM_016103.2	ER-Golgi	v2HS_97583	4	8.5
YKT6	YKT6 v-SNARE homologue	NM_006555.3	SNARE, ER-Golgi transport	v2HS_198177	4	9.3
Early endosome and recycling endosome components						
EEA1	Early endosome antigen 1, 162 kDa	NM_003566.1	Early endosome	v2HS_33005*	16	5.7
				v2HS_33001	4	6.3
RAB21	RAB21, member RAS oncogene family	NM_014999.1	Early endosome	v2HS_96390*	16	5.0
				v2HS_96386*	16	3.8
RAB4A	RAB4A, member RAS oncogene family	NM_004578.2	Endosome recycling	v2HS_244215*	16	6.7
				v2MM_8601	4	4.5
RAB5C	RAB5C, member RAS oncogene family	NM_201434.1	Early endosome	v2MM_83760*	16	7.3
RABEP1	Rabaptin, RAB GTPase binding effector protein 1	NM_004703.3	Endosome recycling	v2HS_37113*	16	12.1
				v2HS_37115*	16	5.5
Exocyst components						
SEC15L1	SEC15-like 1	NM_019053.2	Exocytosis	v2HS_176451*	16	9.0
				v2HS_176449	4	5.3
SEC3L1	SEC3-like 1	NM_178237.1	Exocytosis	v2HS_156567	4	6.5
				v2MM_107535	4	4.5
Late endosome and lysosome proteins						
CTSL	Cathepsin L	NM_001912.2	Lysosomal protease	v2HS_151075*	16	3.8
				v2HS_151070*	16	3.9
				v2HS_151074	4	5.0
				v2HS_151073*	16	4.9
LYST	Chediak–Higashi syndrome 1	NM_000081.2	Lysosomal trafficking	v2HS_88731	4	5.0
				v2HS_88736	4	5.5
VPS28	Vacuolar protein sorting 28	NM_016208.2	Multivesicular body	v2HS_97994*	16	3.6

Increased vacuolar escape by ΔLLO *L. monocytogenes* was determined by counting the number of HEK-293 cells/image filled with GFP-expressing bacteria (escape events). The total number of images analysed is indicated (# images) and the mean number of escape events per image is given (# escaped/image). If the mean number of escape events in shRNA-treated cells was greater than two standard deviations above the mean number of escape events observed in untreated cells (> 3.4 events/image), the shRNA construct is listed in the table. The gene function information is based upon the NCBI Gene database (http://www.ncbi.nlm.nih.gov). Hairpin sequences can be found using the hairpin ID number at http://codex.cshl.edu. Hairpin inserts successfully cloned into the pBS-mir vector are marked with an asterisk (*).
ER, endoplasmic reticulum.

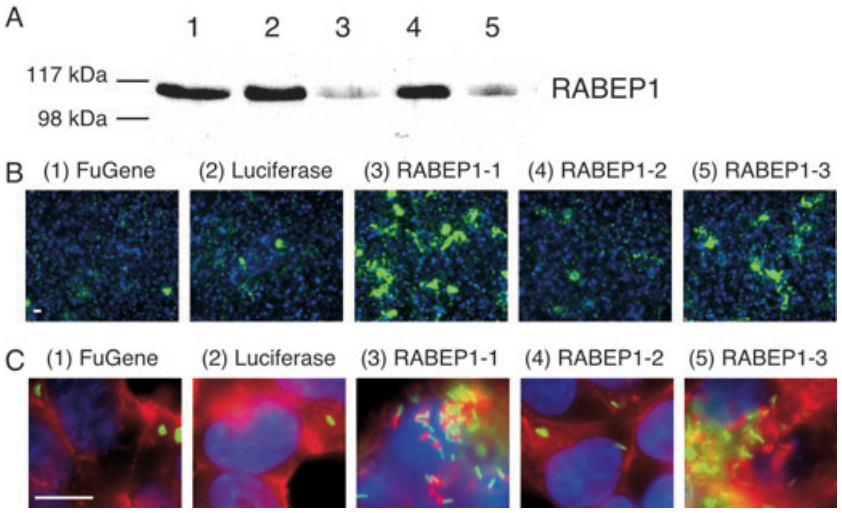

Fig. 2. Knockdown of RABEP1 correlates with increased vacuolar escape.
A and B. 1.0×10^4 HEK-293 cells per well were seeded in a black, clear-bottom 96-well plate. After 24 h, cells were transfected with shRNAs using FuGene 6.
A. Approximately 68 h after transfection, whole-cell extracts were generated and proteins were separated by SDS-PAGE. FuGene 6 alone (lane 1), luciferase shRNA (lane 2), RABEP1-1, RABEP1-2 and RABEP1-3 shRNAs (lanes 3–5). Knockdown efficiency was determined by Western blot using an anti-RABEP1 antibody.
B. Approximately 60 h after transfection, cells were infected with ΔLLO GFP-expressing *L. monocytogenes* (green) at an moi = 5. Gentamicin was added 1 h post infection to kill extracellular bacteria. At 10 h post infection, cells were fixed and host cell nuclei were stained with Hoechst dye (blue). The plates were imaged using automated microscopy at 200× total magnification. Scale bar is 20 μm.
C. 1.0×10^5 HEK-293 cells per well were seeded in a 24-well plate. After 24 h, cells were transfected with shRNAs using FuGene 6. After 48 h, cells were transferred to a 6-well dish containing collagen-coated glass coverslips. Approximately 60 h after transfection, cells were infected with GFP-expressing ΔLLO *L. monocytogenes* (green) at an moi = 5. Gentamicin was added 1 h post infection to kill extracellular bacteria. At 12 h post infection, cells were fixed. Host cell nuclei were stained with Hoechst dye (blue) and host cell actin was stained with Texas-Red phalloidin (red). Cells were imaged at 1000× total magnification. Scale bar is 20 μm.

Loss of bacterial phospholipase activities decreases vacuolar escape efficiency following RABEP1 knockdown

In human cervical epithelial cell lines (HeLa, HEp-2 and Henle 407), the *L. monocytogenes* broad-range phospholipase PC-PLC is required for vacuolar escape in the absence of LLO (Grundling *et al*., 2003). *L. monocytogenes* also encodes a phosphatidylinositol-specific phospholipase, PI-PLC, which assists in lysis of primary vacuoles and double-membrane secondary vacuoles (Smith *et al*., 1995). To determine the roles of the phospholipases for LLO-independent vacuolar escape in HEK-293 cells, we used a GFP-expressing strain lacking LLO and both phospholipases (ΔLLO ΔPI-PLC ΔPC-PLC) as well as GFP-expressing strains lacking LLO and either PI-PLC or PC-PLC (ΔLLO ΔPI-PLC and ΔLLO ΔPC-PLC respectively) to infect HEK-293 cells treated with RABEP1-1 shRNA. PC-PLC was required for the observed increase in vacuolar escape following knockdown of RABEP1 in HEK-293 cells, as infection with ΔLLO ΔPI-PLC ΔPC-PLC or ΔLLO ΔPC-PLC bacteria resulted in no escape events being observed (Fig. 4). PI-PLC was shown to have an important synergistic role in allowing vacuolar escape of ΔLLO *L. monocytogenes* as the ΔLLO ΔPI-PLC strain showed lower levels of vacuolar escape than ΔLLO *L. monocytogenes* (Fig. 4, compare ΔLLO and ΔLLO ΔPI-PLC). Infection of RABEP1-1 shRNA-treated HEK-293 cells with ΔLLO *L. monocytogenes* resulted in ~7.5-fold more escape events per image than infection with ΔLLO ΔPI-PLC *L. monocytogenes* as 34.0 ± 7.1 escape events per image were observed with ΔLLO *L. monocytogenes* infection while 4.5 ± 0.7 escape events per image were observed with ΔLLO ΔPI-PLC *L. monocytogenes* infection.

Knockdown of RABEP1 alters maturation of ΔLLO L. monocytogenes*-containing vacuoles*

The requirement of PC-PLC for vacuolar escape of ΔLLO *L. monocytogenes* provides support for the hypothesis that the increase in vacuolar escape observed following shRNA treatment is due to alterations in vacuole maturation that facilitate function of the bacterial phospholipases. To further characterize the mechanism permitting increased vacuolar escape, we next focused on analysing the effects of knockdown of RABEP1 on the maturation of *L. monocytogenes*-containing vacuoles. We first examined association of LAMP1, a marker of mature/late endosomes and lysosomes, with ΔLLO *L. monocytogenes*.

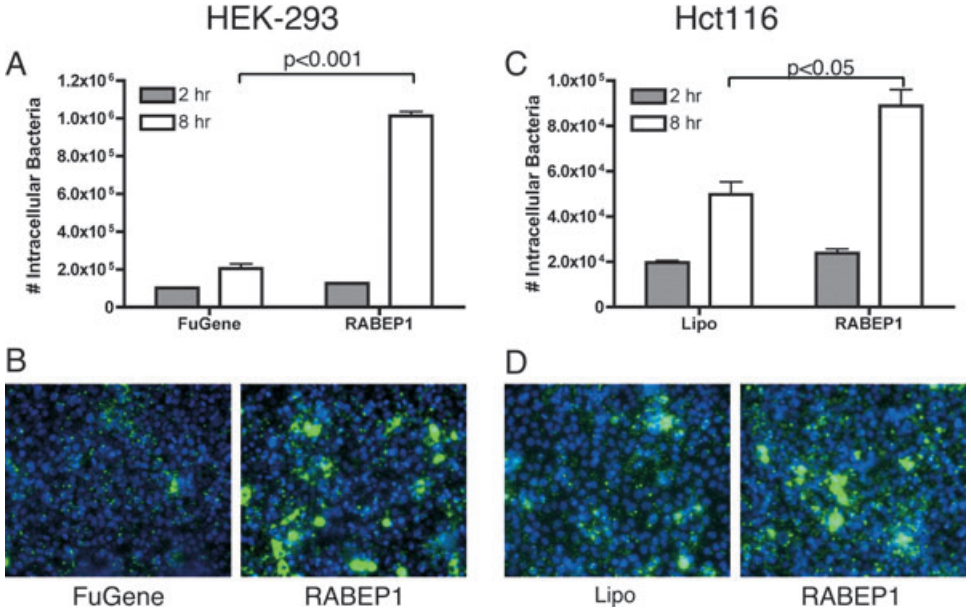

Fig. 3. Knockdown of RABEP1 results in increased vacuolar escape and intracellular replication of ΔLLO *L. monocytogenes* in at least two different human-derived cell lines.
A and B. 1.0×10^4 HEK-293 cells per well were seeded in a black, clear-bottom 96-well plate. Approximately 24 h later, cells were treated with FuGene 6 or transfected with RABEP1-1 shRNA using FuGene 6. Sixty hours after transfection, cells were infected with GFP-expressing ΔLLO *L. monocytogenes* (green) at an moi = 5. Gentamicin was added 1 h post infection to kill extracellular bacteria.
C and D. 1.0×10^5 Hct116 cells per well were seeded in a 24-well plate. Approximately 24 h later, cells were treated with Lipofectamine 2000 (Lipo) or transfected with RABEP1-1 shRNA with Lipofectamine 2000. Approximately 48 h after transfection, the transfected Hct116 cells were resuspended and cells from two wells of the 240well plate were divided and transferred to 10 wells of a black, clear-bottom 96-well plate. After incubating the Hct116 cells for an additional 12 h, the cells were infected with GFP-expressing ΔLLO *L. monocytogenes* at an moi = 5. Gentamicin was added 1 h post infection to kill extracellular bacteria.
A and C. At 2 and 8 h post infection, host cells in three wells per condition were lysed. Appropriate dilutions of the lysates were plated on LB plates and intracellular bacteria were enumerated by counting the number of colony-forming units. Results shown are the means ± SEM of one of three experiments with similar results. *P*-values shown are from a two-tailed Student's *t*-test comparing the number of intracellular bacteria at 8 h post infection.
B and D. At 10 h post infection, cells were fixed and host cell nuclei were stained with Hoechst dye (blue). The plates were imaged using automated microscopy at 200× total magnification. The results shown are representative of at least three independent experiments.

To examine colocalization with LAMP1, we transfected HEK-293 cells with RABEP1-1 shRNA as previously described and then transfected the cells with a LAMP1–CFP fusion construct 24 h prior to infection. Infected HEK-293 cells were fixed and ΔLLO *L. monocytogenes* were detected using wide-field immunofluorescence microscopy. A positive association of LAMP1–CFP with a *L. monocytogenes*-containing vacuole was characterized as a ring of increased CFP fluorescence intensity surrounding the intracellular ΔLLO *L. monocytogenes*.

We initially examined colocalization of LAMP1–CFP with ΔLLO *L. monocytogenes* at 2 h post infection, as phospholipase-mediated vacuolar escape appeared to occur shortly after this time. Colocalization of LAMP1–CFP with ΔLLO *L. monocytogenes* was determined for at least 50 bacteria per transfection condition in each of three independent experiments. In cells treated with FuGene 6 or transfected with firefly luciferase control shRNAs, 79.9% and 82.2% of bacteria, respectively, were positively associated with LAMP1–CFP at 2 h post infection. In cells treated with RABEP1-1 shRNA, a slight decrease in LAMP1–CFP association with ΔLLO *L. monocytogenes* was observed with 71.6% of bacteria associated with LAMP1–CFP. A one-way ANOVA and Bonferronni post tests indicated that RABEP1 knockdown significantly decreased LAMP1–CFP association compared with FuGene 6 ($P < 0.01$) and luciferase ($P < 0.001$) shRNA treatments. There was no statistical difference between FuGene 6 and luciferase shRNA treatments.

Based on the observation of a small, but consistent decrease in the association of ΔLLO *L. monocytogenes* with LAMP1–CFP in cells treated with shRNA targeting RABEP1 at 2 h post infection, we further examined association of LAMP1–CFP with ΔLLO *L. monocytogenes* at various time points post infection. We determined that the association of LAMP1–CFP with intracellular ΔLLO *L. monocytogenes* is significantly decreased at several time points post infection in cells treated with shRNAs targeting RABEP1 (Fig. 5A and B). Association of LAMP1–CFP in control cells and cells treated with shRNAs targeting RABEP1 was similar at 15 min post infection. However, the percentage of LAMP1–CFP

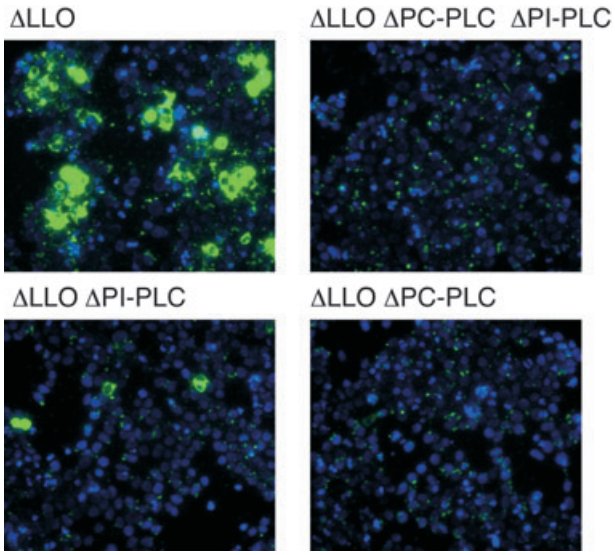

Fig. 4. PC-PLC is required for LLO-independent vacuolar escape. 1.0×10^4 HEK-293 cells per well were seeded in a black, clear-bottom 96-well plate. Approximately 24 h later, cells were transfected with RABEP1-1 shRNAs using FuGene 6. Approximately 60 h after transfection, cells were infected with GFP-expressing *L. monocytogenes* strains (green) at an moi = 5. Gentamicin was added 1 h post infection to kill extracellular bacteria. At 10 h post infection, cells were fixed and host cell nuclei were stained with Hoechst dye (blue). The plates were imaged using automated microscopy at 200× total magnification.

association with ΔLLO *L. monocytogenes* was less in cells treated with RABEP1 shRNA than in control cells at later time points (Fig. 5A). Furthermore, knockdown of RABEP1 primarily had an observable effect on the development of LAMP1-associated phagolysosome-like vacuoles, as the fraction of ΔLLO *L. monocytogenes* associated with the late endosome protein marker RAB7–CFP was not altered following treatment of HEK-293 cells with RABEP1-1 shRNA (Fig. 5C and D). Similarly, the association of the late endosome lipid lysobisphosphatidic acid (LBPA) with ΔLLO *L. monocytogenes* in RABEP1-1 shRNA-treated HEK-293 cells was similar to the association of LBPA with ΔLLO *L. monocytogenes* in control HEK-293 cells (Fig. S1).

Discussion

The observation that ΔLLO *L. monocytogenes* can escape from vacuoles in human-derived cell lines was first made over 20 years ago (Portnoy *et al.*, 1988); however, the mechanism permitting vacuolar escape of ΔLLO bacteria has not been characterized extensively. In this work, we performed a subgenomic RNAi screen in human cells to identify vesicular trafficking factors that play a role in facilitating vacuolar escape of ΔLLO *L. monocytogenes*. Knockdown of 18 different gene products increased vacuolar escape of ΔLLO *L. monocytogenes*. The apparent enhancement of vacuolar escape could be caused by increased bacterial uptake by shRNA-treated host cells or by increased LLO-independent vacuolar dissolution. Quantification of intracellular ΔLLO *L. monocytogenes* at early time points post infection did not show an increase in bacterial uptake following treatment with shRNAs identified in the screen (Fig. 3A and C, Fig. S2 and data not shown). In contrast, the data presented here are consistent with an increased efficiency of vacuolar disruption by ΔLLO *L. monocytogenes* following shRNA treatment. Furthermore, our results suggest that LLO-independent vacuolar dissolution is correlated with reduced vacuolar maturation (Fig. 6).

The bacterial phospholipase PC-PLC was found to be essential for vacuolar escape of ΔLLO *L. monocytogenes* following knockdown of several host cell vesicular trafficking gene products, including RABEP1 (Fig. 4). In recent studies examining the vacuolar biology of *L. monocytogenes*, several different outcomes have been observed depending upon the infection model and how vacuole maturation was altered. In *Drosophila* cells, RNAi knockdown of host cell proteins with roles in lysosomal transport resulted in growth of wild-type and ΔLLO *L. monocytogenes* within vacuoles (Agaisse *et al.*, 2005). Recent work in murine macrophages has shown that LLO can promote replication of *L. monocytogenes* within vacuoles in an autophagy-dependent manner (Birmingham *et al.*, 2008). In both cases, replication within membrane-bound compartments is significantly slower than that observed within the cytosol. In this study, we identified conditions in which phospholipase-mediated vacuolar escape of ΔLLO *L. monocytogenes* occurs at elevated frequencies to allow replication in the cytosol.

Using RNAi in *Drosophila* cells, Portnoy and co-workers determined that knockdown of several components of the MVB and endosomal sorting complex required for transport (ESCRT) complexes allowed bypass of the requirement of LLO for vacuolar escape (Cheng *et al.*, 2005). MVB and ESCRT complexes function in the transition of endosomes to lysosomes. We also observed increased vacuolar escape of ΔLLO *L. monocytogenes* in HEK-293 cells following knockdown of the ESCRT complex member VPS28 (Table 1). In addition to confirming that knockdown of an ESCRT complex subunit can cause increased LLO-independent vacuolar escape within a human cell line, we identified several other functional categories of vesicular trafficking proteins that have roles in facilitating vacuolar escape of ΔLLO *L. monocytogenes* (Table 1). Treatment with shRNAs targeting a lysosomal trafficking protein (LYST) and a lysosomal protease (CTSL) resulted in increased vacuolar escape of ΔLLO bacteria. Knockdown of several members of the COP-I coatomer, a complex involved primarily in Golgi-related vesicle transport (Cai *et al.*, 2007), and

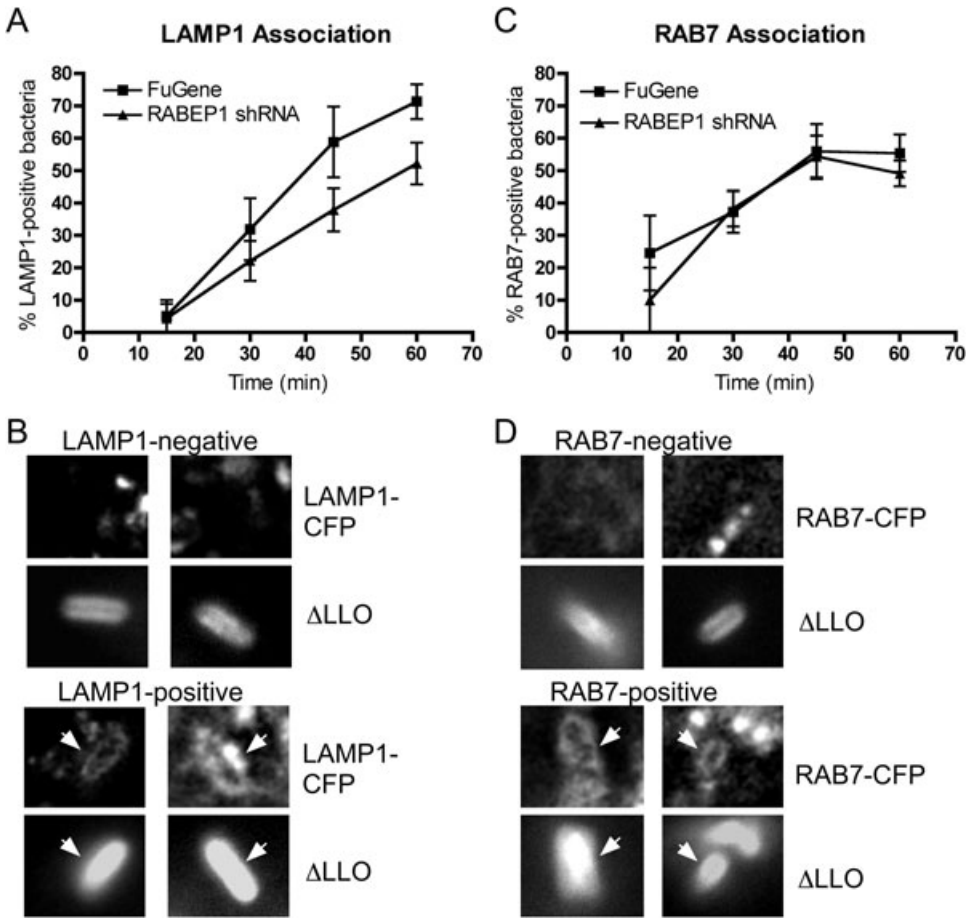

Fig. 5. Association of markers of vacuolar maturation with ΔLLO *L. monocytogenes*.
A. Quantification of LAMP1-positive ΔLLO *L. monocytogenes*. 1.0×10^5 HEK-293 cells were seeded in a 24-well plate. Approximately 24 h later, cells were treated with FuGene 6 or transfected with RABEP1-1 shRNA using FuGene 6. Forty hours later, the cells were subsequently transfected with LAMP1–CFP for 8 h, then transferred to collagen-treated 18 mm coverslips in 6-well dishes for 16 h. The transfected cells were then infected with ΔLLO *L. monocytogenes* at an moi = 50. At the indicated time points post infection, cells were washed extensively and fixed with paraformaldehyde for 16–18 h. Bacteria in cells were stained with an anti-*L. monocytogenes* antibody and Rhodamine Red X-conjugated secondary antibody. Cells were imaged at 1000× total magnification in z-stacks using 0.25 μm z-distance steps. CFP images were processed with deconvolution software prior to analysis. All intracellular bacteria were analysed from at least 10 CFP-transfected cells at each time point in five independent experiments. Results shown are the means ± SEM of all experiments. Differences between FuGene 6 alone and RABEP1-1 shRNA were found to be statistically significant ($P < 0.05$) using a one-tailed paired Student's *t*-test.
B. Representative images taken at various time points of bacteria identified as LAMP1-negative (top) or LAMP1-positive (bottom). Arrows indicate association of LAMP1–CFP with *L. monocytogenes*.
C. Quantification of RAB7-positive bacteria. Transfections, infections, microscopy and data analysis were done as described above except that RAB7–CFP was used instead of LAMP1–CFP. No statistical difference between conditions was observed.
D. Representative images taken at various time points of bacteria identified as RAB7-negative (top) or RAB7-positive (bottom). Arrows indicate association of RAB7–CFP with *L. monocytogenes*.

three additional gene products (RAB2A, SARA2 and YKT6) with roles in endoplasmic reticulum to Golgi vesicular trafficking increased vacuolar escape of ΔLLO *L. monocytogenes*. We also observed increased vacuolar escape following treatment with shRNAs targeting two exocyst components, SEC3L1 and SEC15L1. The exocyst complex is required for protein secretion and functions in vesicle transport between the Golgi apparatus, endosomes and the plasma membrane (Wang and Hsu, 2006). Two other functional categories of gene products that when targeted by shRNA treatment caused increased LLO-independent vacuolar escape were those involved in regulation and formation of early endosomes and recycling endosomes. These results suggest that several vesicular trafficking pathways can be altered in human cells that permit efficient intracellular infection by ΔLLO *L. monocytogenes*.

Previous work has suggested that vacuolar escape of *L. monocytogenes* is inhibited by maturation of vacuoles to lysosome-like compartments. Mature LAMP1-positive vacuoles are not as permissive for vacuolar escape of *L. monocytogenes* (Henry *et al.*, 2006). Additionally, the

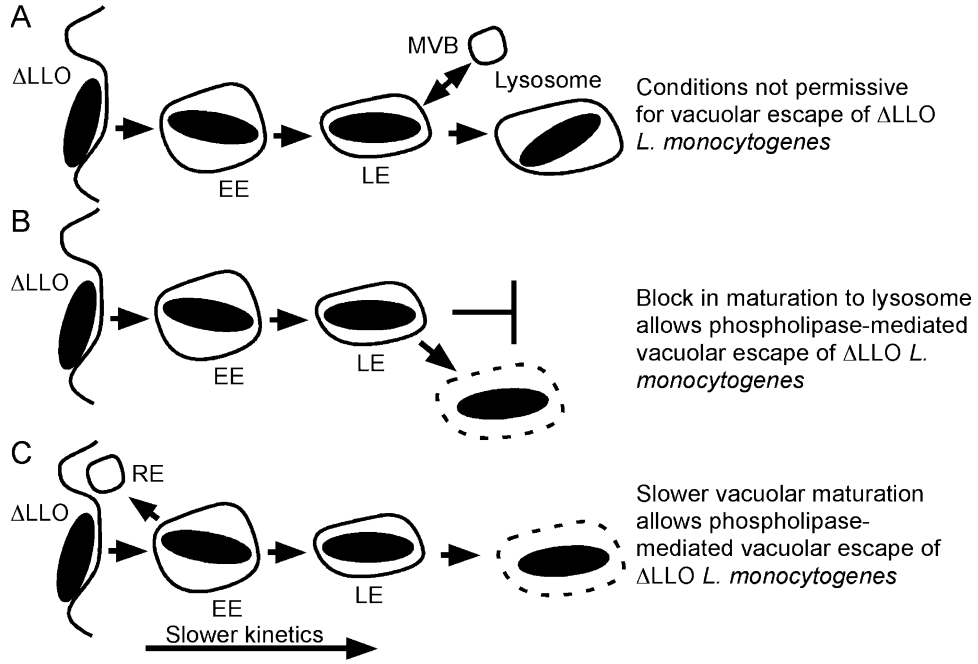

Fig. 6. Model of phospholipase-mediated LLO-independent vacuolar escape.
A. After entry of ΔLLO *L. monocytogenes* into vacuoles resembling early endosomes (EE), ΔLLO *L. monocytogenes*-containing vacuoles undergo maturation to late endosome-like (LE) and to lysosome-like structures. Maturation to lysosome-like structures involves interactions of the vacuole with multivesicular bodies (MVB). The maturation is not slowed by LLO-mediated perforations that uncouple pH and calcium gradients acting as signals for vacuolar maturation. Once the vacuole has matured to a lysosome-like compartment, the bacterial phospholipases cannot mediate vacuole escape.
B. ΔLLO *L. monocytogenes*-containing vacuoles undergo maturation to LE, but when further maturation is blocked by knockdown of host MVB or lysosomal proteins, the bacteria remain in LE compartments favorable for phospholipase activity and eventual vacuole escape.
C. ΔLLO *L. monocytogenes*-containing vacuoles undergo maturation to LE, but the maturation process is slowed by knockdown of host vesicular trafficking proteins required for efficient vacuole maturation. Knockdown of recycling endosome (RE) components may alter vacuolar maturation. As a result, the bacteria remain in LE compartments favourable for phospholipase activity for a longer period of time permitting phospholipase-mediated vacuole escape.

lysosomal protease cathepsin-D has been implicated in degrading LLO and inhibiting *L. monocytogenes* intracellular growth (del Cerro-Vadillo *et al*., 2006). Moreover, Cheng *et al*. (2005) suggested that knockdown of MVB components allowed increased vacuolar escape of ΔLLO *L. monocytogenes* in *Drosophila* cells due to a block of vacuolar maturation. Our results examining vacuolar maturation following knockdown of the early endosome/recycling endosome regulator RABEP1 support the hypothesis that LLO-independent vacuolar escape is inversely correlated with rates of vacuolar maturation. In five independent experiments, we showed a decreased association of the lysosomal protein LAMP1 with ΔLLO *L. monocytogenes*-containing vacuoles following knockdown of RABEP1 (Fig. 5A). While the transfection procedure used allowed for a limited number of host cells to be evaluated per experiment, the data were consistent and suggest that knockdown of RABEP1 alters the maturation of ΔLLO *L. monocytogenes*-containing vacuoles and results in increased vacuolar escape of ΔLLO *L. monocytogenes* (Fig. 5A).

Our analysis of the maturation of ΔLLO *L. monocytogenes* vacuoles in cell lines in which varying levels of LLO-independent vacuolar escape occurs also suggests that LLO-independent vacuolar dissolution may be inversely correlated with rates of vacuolar maturation. Swanson and co-workers previously showed that 90% of vacuoles containing ΔLLO *L. monocytogenes* were LAMP1-positive by 15 min post infection in RAW 264.7 cells (Henry *et al*., 2006), a cell line where vacuolar escape is absolutely dependent upon LLO. We determined that in HEK-293 cells, where ΔLLO *L. monocytogenes* can undergo vacuolar escape at a low frequency, ~5% of intracellular ΔLLO *L. monocytogenes* were LAMP1-postive 15 min post infection (Fig. 5A). In HEK-293 cells, ΔLLO *L. monocytogenes* vacuoles eventually mature to lysosomes, but the association of LAMP1 occurs at later time points. The percentage of ΔLLO *L. monocytogenes* associated with LAMP1 in HEK-293 cells increases from ~5% LAMP1-positive vacuoles 15 min post infection to a maximum of ~80% LAMP1-positive vacuoles at 2 h post infection. The efficiency of

vacuolar maturation and the vacuolar escape efficiency of ΔLLO *L. monocytogenes* appear to be correlated in murine RAW 264.7 macrophage cells and in human HEK-293 epithelial cells. In human HEp-2 cervical epithelial cells, ΔLLO *L. monocytogenes* escape the vacuole efficiently (Grundling *et al*., 2003). Consistent with the correlation that LLO-independent vacuolar escape occurs more readily in cells with slower vacuolar maturation rates, preliminary results suggest that LAMP1 association with ΔLLO *L. monocytogenes* is much slower in HEp-2 cells than in HEK-293 cells yielding ~18% LAMP1-positive vacuoles in HEp-2 cells 60 min post infection compared with ~70% LAMP1-positive vacuoles in HEK-293 cells 60 min post infection (data not shown and Fig. 5A).

Our results suggest that knockdown of host cell vesicular trafficking proteins within each of the identified functional categories (Table 1) could result in a block in vacuolar maturation or a general slowing of vacuolar maturation (Fig. 6). Enhanced vacuolar dissolution following knockdown of MVB components and lysosomal proteins is likely due to blocking the formation of a degradative, LAMP1-positive, lysosomal compartment (Piper and Katzmann, 2007). Interestingly, knockdown of ESCRT complex members in *Drosophila* S2 cells and murine RAW 264.7 macrophage-like cells was recently shown to make cells permissive for intracellular infection by normally non-pathogenic *Mycobacterium smegmatis* (Philips *et al*., 2008). Knockdown of ESCRT complexes also prevented expression of GFP from an acid-activated promoter in *M. fortuitum* indicating that knockdown of ESCRT complexes resulted in the bacteria residing in a less acidic, less mature vacuolar compartment (Philips *et al*., 2008). Knockdown of COP-I coatomer subunits may be disrupting protein trafficking from the Golgi apparatus to the endoplasmic reticulum and between Golgi cisternae resulting in pleiotropic effects on vesicle dynamics within the cell. However, knocking down COP-I components may result in a more specific inhibition of vacuolar maturation, as some subunits of the COP-I complex have been localized to endosomes and have functional roles in the formation of vesicles that allow transport between early and late endosomes (Aniento *et al*., 1996). Exocyst components have been recently identified as being associated with phagosomes in *Drosophila* cells and murine macrophages (Stuart *et al*., 2007). We hypothesize that exocyst components may also be a part of the induced phagosome-like vacuoles formed to allow *L. monocytogenes* uptake in non-professional phagocytic cells, such as epithelial cells, and that these proteins may function in the maturation of the vacuole, perhaps by assisting in the removal of proteins associated with early stages of maturation. Knockdown of early endosome or recycling endosome components likely affect the vacuole protein composition early after bacterial entry. These altered vacuoles may be missing signalling proteins required for acquisition of late endosome and lysosomal characteristics. Indeed, inhibition of endosome recycling by expression of a dominant negative version of RAB11 has previously been shown to slow maturation of *Salmonella*-containing vacuoles (Smith *et al*., 2005).

Slower vacuolar maturation may be more permissive for efficient vacuolar escape of *L. monocytogenes* for multiple reasons. First, slower vacuolar maturation may provide the bacterial phospholipases with an environment more conducive for optimal activity for a longer period of time. It is known that PC-PLC activity is activated at pH 7.0 and lower, but not at pH 7.3 (Marquis and Hager, 2000). Therefore, slightly acidic endosome-like compartments are likely to promote activation of PC-PLC, but do not contain the high concentrations of degradative proteases found in more mature lysosomal compartments. The concept that lysosomal compartments are inhibitory for *L. monocytogenes* protein function is supported by the observation that wild-type *L. monocytogenes* escape inefficiently from LAMP1-positive lysosomal vacuoles (Henry *et al*., 2006). Also, as *plcA* and *plcB*, the genes encoding PI-PLC and PC-PLC, are upregulated during intracellular infection (Chatterjee *et al*., 2006), the altered vacuolar maturation may allow for the bacteria to produce increased levels of the phospholipases before the vacuole matures to a degradative lysosomal compartment. Additionally, there may be differences in the membrane composition of the endosome-like *L. monocytogenes* vacuoles that are better substrates for PC-PLC. Conditions that increase vacuolar escape of ΔLLO *L. monocytogenes* do not alter the concentration of the late endosome-specific lipid LBPA in the vacuolar membrane (Fig. S1), but the concentrations of other phospholipids may affect LLO-independent vacuolar escape efficiencies. PC-PLC is a broad-range phospholipase, but has been shown to have higher levels of activity on vesicles containing phosphatidylserine and phosphatidylethanolamine than on sphingomyelin and phosphatidylcholine containing membranes (Montes *et al*., 2004). The relative levels of these phospholipids may be altered by changes in vesicular trafficking (Yeung and Grinstein, 2007).

Our results suggest that knockdown of RABEP1 altered LAMP1 acquisition on ΔLLO *L. monocytogenes*-containing vacuoles in HEK-293 cells (Fig. 5A). However, we did not observe differences in the late endosome stage of vacuolar maturation either when measuring RAB7 or LBPA association with intracellular ΔLLO *L. monocytogenes* following treatment with shRNAs targeting RABEP1 (Fig. 5C and Fig. S1). We initially found this result surprising as RAB7 generally functions at an intermediate step between early endosomes and lyso-

somes. One possible explanation is that as the late endosome stage is transient, while mature LAMP1 vacuoles persist in cells, the changes in maturation are simply not sufficient to observe a difference at the late endosome stage. Another possibility is that, as RABEP1 functions at the junction of whether endosomes are recycled or mature, knockdown of RABEP1 may alter endosome formation and shift the balance towards recycling endosome-like compartments while simultaneously slowing down the maturation process of endosomes (Deneka *et al*., 2003). This phenotype would result in fewer *L. monocytogenes* vacuoles becoming late endosome-like, but with those still formed having slower kinetics of LAMP1 acquisition. When RAB7 association was examined at fixed time points, the reduced formation efficiency and increased duration of the late endosome-like stage may result in approximately the same fraction of membrane-bound compartments being RAB7-positive as in control cells.

RABEP1 is a Rab effector protein that has been shown to interact with both RAB4A and RAB5A to regulate passage of cargo in early endosomes to either the recycling pathway (back to the surface or Golgi) or the endocytic maturation pathway (towards lysosomes) (Deneka *et al*., 2003; Pagano *et al*., 2004). RAB4A was also identified in our RNAi screen (Table 1). Furthermore, murine Rab5a has been implicated in regulating *L. monocytogenes* infection and the *L. monocytogenes* p40 protein has been shown to inhibit Rab5a GDP/GTP exchange activity (Alvarez-Dominguez *et al*., 2008). Degradation of RABEP1 by caspase-3 following infection with *L. pneumophila* has also been implicated in halting maturation of the *Legionella*-containing vacuole (LCV) (Molmeret *et al*., 2004). Collectively, these data suggest that the switch between endosome maturation and endosome recycling may be important for modulating the *L. monocytogenes* vacuole, both in our infection conditions where LLO is absent and during wild-type infections. The importance of the regulation of endosome recycling during *L. monocytogenes* infection and for the proper formation of *Salmonella*-containing vacuoles and *Legionella*-containing vacuoles suggests that modifications of endosome recycling may alter vacuolar maturation during infection by a variety of intracellular pathogens. In *L. monocytogenes* infections, LLO has been shown to slow vacuolar maturation kinetics by uncoupling pH and calcium gradients that act as maturation signals (Shaughnessy *et al*., 2006). Our work demonstrating that knockdown of host cell factors resulting in altered vacuolar maturation can compensate for the vacuolar escape defect of ΔLLO *L. monocytogenes* suggests that the ability of LLO to slow vacuolar maturation is functionally important during infection.

Experimental procedures

L. monocytogenes *strains and growth conditions*

Listeria monocytogenes strains used in this study were 10403S ΔLLO (DH-L489), pPL3-bGFP ΔLLO (DH-L1288), pPL3-bGFP ΔLLO ΔPI-PLC ΔPC-PLC (DH-L1546), pPL3-bGFP ΔLLO ΔPI-PLC (DH-L1544) and pPL3-bGFP ΔLLO ΔPC-PLC (DH-L1545). pPL3-bGFP is a pPL3-based integration vector (Grundling *et al*., 2004) that expresses GFPmut2 from the $tRNA^{Arg}$ locus on the *L. monocytogenes* chromosome. gfp_{mut2} in pPL3-bGFP is transcribed from the constitutive pHyper promoter as a fusion to the 5′ UTR of the *L. monocytogenes hly* gene (Shen and Higgins, 2005). *L. monocytogenes* strains were routinely grown at 37°C in brain heart infusion (BHI) broth or on BHI agar (Difco Laboratories, Detroit, MI). *L. monocytogenes* were typically grown in 2 ml BHI at 30°C without shaking for 14–16 h prior to infection. All *L. monocytogenes* strains were stored at −80°C in BHI containing 40% glycerol. Chloramphenicol was used at 7.5 μg ml^{-1} for selection of integrated pPL3 derivatives in *L. monocytogenes*.

Tissue culture cell growth conditions

HEK-293 human kidney epithelial cells (ATCC CRL-1573) and Hct116 human colon epithelial cells (ATCC CCL-247) were cultured in Dulbecco's modified Eagle's medium (DMEM; Mediatech, Herndon, VA) supplemented with 10% fetal bovine serum (HyClone, Logan, UT), 2 mM glutamine, 1 mM sodium pyruvate and 100 μg ml^{-1} penicillin and streptomycin (P/S) (DMEM-10-P/S). For infection assays, host cell cultures were maintained in antibiotic-free DMEM-10 medium (DMEM-10). All host cell cultures were maintained at 37°C in a 5% CO_2-air atmosphere.

shRNA constructs and library

Escherichia coli clones containing the pSMC2 shRNAs were isolated from the human genome library described in Silva *et al*. (2005) and grown in Luria–Bertani (LB) with 40 μg ml^{-1} chloramphenicol. Aliquots were frozen in 20% glycerol at −80°C and shRNA plasmids were prepared using a 96-well mini-prep kit (Qiagen, Valencia, CA). Plasmid concentrations were tested from representative wells and were approximately 200 ng μl^{-1}. For sequencing, additional plasmid DNA was prepared from 5 ml cultures started from the frozen aliquots using a single-column mini-prep kit (Qiagen). Sequences for all hairpin inserts listed in Table 1 can be found at http://codex.cshl.org. Mating was used to move shRNA inserts from the pSMC2 shRNA vector to the pBS-mir vector and was done as previously described (Li and Elledge, 2005).

RNAi screen and secondary infections in HEK-293 cells

1.0×10^4 HEK-293 cells per well were seeded in a black, clear-bottom 96-well plate (Corning, Lowell, MA) in 100 μl DMEM-10. Twenty-four hours later, cells were transfected with shRNAs using FuGene 6 (Roche Diagnostics, Basel, Switzerland). For transfection of each well, 0.6 μl FuGene 6 was diluted in 20 μl OPTI-MEM, followed by addition of approximately 0.2 μg shRNA plasmid DNA and incubation for 20 min at room temperature

(RT; 20–25°C). Complexes were added to cells and plates were centrifuged for 5 min at 200 *g* in a table-top centrifuge. Approximately 60 h after transfection, cells were infected with GFP-expressing *L. monocytogenes* strains at a multiplicity of infection (moi) = 5 by addition of bacteria in 25 µl DMEM-10, followed by centrifuging the plates for 1 min at 200 *g*. Twenty-five microlitres of DMEM-10 with 350 µg ml^{-1} gentamicin was added 1 h post infection to kill extracellular bacteria (final concentration of 50 µg ml^{-1} gentamicin). At 10 h post infection, cells were fixed with 3.2% paraformaldehyde in phosphate-buffered saline (PBS), pH 7.1 for 14–18 h at 4°C. Host cell nuclei were then stained with Hoechst dye by washing wells once with PBS, incubating cells for 15 min at RT with 1:5000 Hoechst 33342 (Invitrogen, Carlsbad, CA) in PBS-0.1% Triton X-100 and washing once with PBS. The plates were imaged using automated microscopy at DAPI and FITC wavelengths at 200× total magnification. Automated microscopy was performed as previously described (Agaisse *et al.*, 2005).

HEK-293 intracellular growth assays

The infections for the secondary RNAi screens were performed as described above; however, at 2 h post infection and 8 h post infection cells from three wells of each shRNA treatment were lysed in 100 µl PBS + 0.1% Triton X-100. Intracellular bacteria from the lysed cells were diluted in PBS and plated on LB agar at 37°C. After 24 h, the number of colony-forming units was determined.

Phalloidin staining for actin association with cytosolic bacteria

1.0×10^5 HEK-293 cells per well were seeded in a 24-well plate. After 24 h, cells were transfected with shRNAs using FuGene 6. After 48 h, cells were transferred to a 6-well dish containing collagen-coated glass coverslips. Approximately 60 h after transfection, cells were infected with GFP-expressing ΔLLO *L. monocytogenes* at an moi = 5 in 2 ml DMEM-10. Cells were washed with PBS and DMEM-10 with 50 µg ml^{-1} gentamicin was added 1 h post infection to kill extracellular bacteria. At 12 h post infection, cells were fixed with 3.2% paraformaldehyde in PBS. Fixed coverslips were washed with Tris-buffered saline (TBS), pH 8.0 supplemented with 0.1% Triton X-100 (TBS-TX) and stained for 30 min with 33 nM Texas-Red phalloidin (Molecular Probes, Eugene, OR) in TBS-TX supplemented with 1% BSA. Following an additional wash, samples were stained with Hoechst 33342 (Molecular Probes, Eugene, OR) in TBS-TX for 10 min. Coverslips were washed with TBS-TX and mounted with mounting media containing 20 mM Tris pH 8.0, 0.5% N-propyl gallate (Sigma) and 90% glycerol. Cells were imaged with a TE-300 inverted microscope (Nikon Instruments, Melville, NY) and 100× Plan Fluor objective using MetaMorph (Molecular Devices, Downington, PA) software for image acquisition and analysis.

Hct116 infections and intracellular growth assays

1.0×10^5 Hct116 cells per well were seeded in a 24-well tissue culture plate in 500 µl DMEM-10. Twenty-four hours later, cells were transfected with shRNAs using Lipofectamine 2000 (Invitrogen). For transfection of each well, 1.5 µl Lipofectamine 2000 was diluted in 50 µl OPTI-MEM and incubated at RT for 5 min. 0.5 µg shRNA plasmid DNA was diluted in 50 µl OPTI-MEM aliquots, then 50 µl of Lipofectamine 2000 mixture was added to each shRNA plasmid mixture followed by a 20 min incubation at RT. Complexes were added to cells and plates rocked to mix. Approximately 48 h after transfection, cells were resuspended in 1.5 ml DMEM-10. For microscopy infections, 100 µl/well of cells were seeded in wells of a black, clear-bottom 96-well plate. For intracellular growth assays, 500 µl/well of cells were seeded in wells of a 24-well plate. Cells were incubated for 12 h, then infected with GFP-expressing *L. monocytogenes* strains at an moi = 5. For microscopy infections, bacteria were added in 25 µl DMEM-10, followed by centrifuging plates for 1 min at 200 *g*. Twenty-five microlitres of DMEM-10 with 350 µg ml^{-1} gentamicin was added 1 h post infection to kill extracellular bacteria (final concentration of 50 µg ml^{-1} gentamicin). At 10 h post infection, cells were fixed with 3.2% paraformaldehyde in PBS for 14–18 h at 4°C. Host cell nuclei were stained with Hoechst dye by washing wells once with PBS, incubating cells for 15 min at RT with 1:5000 Hoechst 33342 in PBS-0.1% Triton X-100 and washing once with PBS. The plates were imaged using automated microscopy at DAPI and FITC wavelengths at 200× total magnification. For intracellular growth assays, media were removed from wells and bacteria were added in 500 µl DMEM-10, followed by centrifuging plates for 1 min at 200 *g*. At 1 h post infection, media with bacteria were removed and 500 µl of DMEM-10 with 50 µg ml^{-1} gentamicin was added. At 2 h post infection and 8 h post infection, cells from three wells of each shRNA treatment were lysed in 500 µl PBS + 0.1% Triton X-100. Intracellular bacteria from the lysed cells were diluted in PBS and plated on LB agar at 37°C. After 24 h, the number of colony-forming units was determined.

Analysis of RABEP1 knockdown

HEK-293 cells were transfected as described above in a 96-well plate. Protein samples were prepared by first resuspending cells from one well in 100 µl cold PBS and then pelleting at 800 *g*, 5 min, at 4°C. Cells were lysed by resuspending the pellet in lysis buffer (420 mM KCl, 50 mM Hepes, pH 8.3, 1 mM EDTA, 0.1% NP-40), incubating on ice for 15 min and pelleting the cell debris at 16 000 *g*, 10 min, at 4°C. Total protein concentrations were determined using a Bradford assay (Sigma, St Louis, MO) and equal amounts of whole-cell lysate proteins were loaded in each well of an SDS-PAGE gel. Proteins were separated, transferred to PVDF membranes and Western blots were performed using a rabbit anti-RABEP1 antibody (Santa Cruz Biotechnology, Santa Cruz, CA) and mouse anti-actin antibodies (Sigma) as a loading control. HRP-conjugated anti-rabbit and anti-mouse antibodies were used to detect primary antibodies (Bio-Rad, Hercules, CA).

Microscopy analysis of CFP-labelled markers of vacuolar maturation

1.0×10^5 HEK-293 cells were seeded in a 24-well plate in 500 µl DMEM-10. Twenty-four hours later, cells were treated

with FuGene 6 or transfected with luciferase or RABEP1-1 shRNA using FuGene 6 for 40 h, then transfected with LAMP1–CFP plasmid (JS106) or RAB7–CFP plasmid (JS036) DNA (Henry *et al*., 2006) for 8 h, then transferred to collagen-treated 18 mm coverslips in 6-well dishes for 16 h. The transfected cells were then infected with ΔLLO *L. monocytogenes* grown at 30°C for 3 h ($OD_{600} = 0.5$) at an moi = 50 in 2 ml DMEM-10. Bacteria were centrifuged onto cells at 600 *g* for 5 min at RT. For infections of 60 min of less, cells were washed extensively and cells were fixed with 3.2% paraformaldehyde in PBS at indicated time points post infection. For the 2 h infections, cells were washed with PBS at 60 min post infection and DMEM-10 with 50 μg ml^{-1} gentamicin was added to kill extracellular bacteria. At 2 h post infection, cells were fixed in 3.2% paraformaldehyde in PBS. Cells from all infections were fixed for 16–18 h. Bacteria in cells were stained with a rabbit anti-*L. monocytogenes* antibody (Difco) and Rhodamine Red X-conjugated donkey anti-rabbit IgG secondary antibody (Jackson ImmunoResearch, West Grove, PA). Coverslips were mounted with mounting media containing 20 mM Tris pH 8.0, 0.5% N-propyl gallate (Sigma) and 90% glycerol. Cells were imaged with a Nikon TE-2000 inverted microscope using CFP and RFP filter sets with a 100× Plan Apo 1.4 NA objective in z-series with 0.25 μm z-steps according to the recommended Nyquist z-sampling distance. Images were acquired using MetaMorph software. CFP images were processed with AutoDeblur deconvolution software using adaptive (blind) point spread function prior to analysis (MediaCybernetics, Bethesda, MD). Bacteria were determined to be CFP-positive if there was a region of enrichment (defined as increased fluorescence intensity) encircling the location of the bacteria in the CFP images. In establishing the criteria for CFP-positive bacteria, we measured pixel intensity of regions immediately surrounding the bacteria and regions in random locations throughout the cell. Additionally, to check accuracy, other individuals scored selected images without knowledge of the experimental condition of the images. Quantitative results are presented as the mean ± SEM. For the 2 h infections, approximately 50 intracellular bacteria were examined for each condition in at least three independent experiments. The total numbers of intracellular bacteria counted were as follows: 216 (FuGene), 139 (Luciferase shRNA) and 176 (RABEP1 shRNA). For the 60 min time-course experiment, all intracellular bacteria were examined from at least 10 CFP-transfected cells at each time point for each vacuolar maturation marker in five independent experiments. The total numbers of intracellular bacteria counted for the LAMP1–CFP experiments with FuGene treatment were: 19 (15 min), 49 (30 min), 56 (45 min) and 99 (60 min). For the LAMP1–CFP experiments with RABEP1 shRNA treatment the numbers counted were: 25 (15 min), 45 (30 min), 65 (45 min) and 80 (60 min). The total numbers of intracellular bacteria counted for the RAB7–CFP experiments with FuGene treatment were: 40 (15 min), 51 (30 min), 73 (45 min) and 119 (60 min). For the RAB7–CFP experiments with RABEP1 shRNA treatment the numbers counted were: 15 (15 min), 51 (30 min), 76 (45 min) and 106 (60 min).

Microscopy analysis of LBPA

1.0×10^5 HEK-293 cells were seeded in a 24-well plate in 500 μl DMEM-10. Twenty-four hours later, cells were treated with FuGene 6 or transfected with RABEP1-1 shRNA using FuGene 6 for 60 h, then transferred to collagen-treated 18 mm coverslips in 6-well dishes for 16–18 h. The transfected cells were then infected with ΔLLO *L. monocytogenes* grown at 30°C for 3 h ($OD_{600} = 0.5$) at an moi = 50 in 2 ml DMEM-10. Bacteria were centrifuged onto cells at 600 *g* for 5 min at RT. For infections of 60 min or less, cells were washed extensively and fixed with 3.2% paraformaldehyde in PBS at the indicated time points post infection. For the 2 h infections, cells were washed with PBS at 60 min post infection and DMEM-10 with 50 μg ml^{-1} gentamicin was added to kill extracellular bacteria. At 2 h post infection, cells were fixed in 3.2% paraformaldehyde in PBS. Cells from all infections were fixed for 16–18 h at 4°C. Any remaining extracellular bacteria were stained without cell permeabilization in PBS + 0.1% BSA with a rabbit anti-*L. monocytogenes* antibody (Difco) and goat anti-rabbit IgG AlexaFluor350-conjugated secondary antibody (Invitrogen). Following extensive washing, the cells were permeabilized with saponin buffer and stained for intracellular *L. monocytogenes* and LBPA simultaneously. First, cells were incubated with rabbit anti-*L. monocytogenes* antibody and mouse anti-LBPA antibody (Kobayashi *et al*., 1998) in PBS + 0.05% saponin (for permeabilization). After washing with PBS, cells were incubated with donkey anti-rabbit IgG FITC-conjugated secondary antibody (Jackson ImmunoResearch) and donkey anti-mouse Rhodamine Red X-conjugated secondary antibody (Jackson ImmunoResearch) in PBS. Coverslips were mounted with mounting media containing 20 mM Tris, pH 8.0, 0.5% N-propyl gallate (Sigma) and 90% glycerol. Cells were imaged with a Nikon TE-2000 inverted microscope with a 100× Plan Apo objective in z-series with 0.25 μm z-distance steps using DAPI (AlexaFluor 350), FITC and Texas Red filter sets. Images were acquired using MetaMorph software. AlexaFluor 350-negative (intracellular) bacteria were determined to be LBPA-positive if there was a region of enrichment (defined as increased fluorescence intensity) encircling the location of the bacteria in the Texas Red images. All intracellular bacteria were analysed from at least 20 host cells at each time point in four independent experiments. The total numbers of intracellular bacteria counted for the LBPA experiments with FuGene treatment were: 75 (30 min), 155 (60 min) and 162 (120 min). For the LBPA experiments with RABEP1 shRNA treatment the numbers counted were: 67 (15 min), 153 (30 min) and 146 (60 min).

Acknowledgements

We thank current and past members of the Higgins lab for helpful discussions, especially Heather Kamp and Christine Alberti-Segui. We would also like to thank Jing Chen for assistance with the construction of the vesicular trafficking shRNA library and Jianping Jin for construction of the pBS-mir vector. We thank Dr Joel Swanson for the kind gift of LAMP1–CFP and RAB7–CFP constructs and Dr Jean Gruenberg for making the LBPA antibody available to us. Microscopy images to determine the association of markers of vacuolar maturation for this study were acquired and analysed in the Nikon Imaging Center at Harvard Medical School. We would like to thank the imaging centre staff for their advice and assistance. This work was supported by U.S. Public Health Service Grants AI-053669 and AI-056446 (D.E.H.) and Grant AG-011085 (J.W.H.) from the National Institutes of Health.

L.S.B. was a Howard Hughes Medical Institute Predoctoral Fellow.

References

Agaisse, H., Burrack, L.S., Philips, J.A., Rubin, E.J., Perrimon, N., and Higgins, D.E. (2005) Genome-wide RNAi screen for host factors required for intracellular bacterial infection. *Science* **309:** 1248–1251.

Alberti-Segui, C., Goeden, K.R., and Higgins, D.E. (2007) Differential function of *Listeria monocytogenes* listeriolysin O and phospholipases C in vacuolar dissolution following cell-to-cell spread. *Cell Microbiol* **9:** 179–195.

Alvarez-Dominguez, C., Madrazo-Toca, F., Fernandez-Prieto, L., Vandekerckhove, J., Pareja, E., Tobes, R., *et al.* (2008) Characterization of a *Listeria monocytogenes* protein interfering with Rab5a. *Traffic* **9:** 325–337.

Aniento, F., Gu, F., Parton, R.G., and Gruenberg, J. (1996) An endosomal beta COP is involved in the pH-dependent formation of transport vesicles destined for late endosomes. *J Cell Biol* **133:** 29–41.

Beauregard, K.E., Lee, K.D., Collier, R.J., and Swanson, J.A. (1997) pH-dependent perforation of macrophage phagosomes by listeriolysin O from *Listeria monocytogenes*. *J Exp Med* **186:** 1159–1163.

Birmingham, C.L., Canadien, V., Kaniuk, N.A., Steinberg, B.E., Higgins, D.E., and Brumell, J.H. (2008) Listeriolysin O allows *Listeria monocytogenes* replication in macrophage vacuoles. *Nature* **451:** 350–354.

Cai, H., Reinisch, K., and Ferro-Novick, S. (2007) Coats, tethers, Rabs, and SNAREs work together to mediate the intracellular destination of a transport vesicle. *Dev Cell* **12:** 671–682.

Camilli, A., Tilney, L.G., and Portnoy, D.A. (1993) Dual roles of *plcA. Listeria monocytogenes* pathogenesis. *Mol Microbiol* **8:** 143–157.

del Cerro-Vadillo, E., Madrazo-Toca, F., Carrasco-Marin, E., Fernandez-Prieto, L., Beck, C., Leyva-Cobian, F., *et al.* (2006) Cutting edge: a novel nonoxidative phagosomal mechanism exerted by cathepsin-D controls *Listeria monocytogenes* intracellular growth. *J Immunol* **176:** 1321–1325.

Chatterjee, S.S., Hossain, H., Otten, S., Kuenne, C., Kuchmina, K., Machata, S., *et al.* (2006) Intracellular gene expression profile of *Listeria monocytogenes*. *Infect Immun* **74:** 1323–1338.

Cheng, L.W., and Portnoy, D.A. (2003) *Drosophila* S2 cells: an alternative infection model for *Listeria monocytogenes*. *Cell Microbiol* **5:** 875–885.

Cheng, L.W., Viala, J.P., Stuurman, N., Wiedemann, U., Vale, R.D., and Portnoy, D.A. (2005) Use of RNA interference in *Drosophila* S2 cells to identify host pathways controlling compartmentalization of an intracellular pathogen. *Proc Natl Acad Sci USA* **102:** 13646–13651.

Deneka, M., Neeft, M., Popa, I., van Oort, M., Sprong, H., Oorschot, V., *et al.* (2003) Rabaptin-5alpha/rabaptin-4 serves as a linker between rab4 and gamma(1) -adaptin in membrane recycling from endosomes. *Embo J* **22:** 2645–2657.

Derre, I., Pypaert, M., Dautry-Varsat, A., and Agaisse, H. (2007) RNAi screen in *Drosophila* cells reveals the involvement of the Tom complex in *Chlamydia* infection. *Plos Pathog* **3:** 1446–1458.

Dorer, M.S., Kirton, D., Bader, J.S., and Isberg, R.R. (2006) RNA interference analysis of *Legionella* in *Drosophila* cells: exploitation of early secretory apparatus dynamics. *PLoS Pathog* **2:** e34.

Edelson, B.T., and Unanue, E.R. (2001) Intracellular antibody neutralizes *Listeria* growth. *Immunity* **14:** 503–512.

Glomski, I.J., Gedde, M.M., Tsang, A.W., Swanson, J.A., and Portnoy, D.A. (2002) The *Listeria monocytogenes* hemolysin has an acidic pH optimum to compartmentalize activity and prevent damage to infected host cells. *J Cell Biol* **156:** 1029–1038.

Grundling, A., Gonzalez, M.D., and Higgins, D.E. (2003) Requirement of the *Listeria monocytogenes* broad-range phospholipase PC-PLC during infection of human epithelial cells. *J Bacteriol* **185:** 6295–6307.

Grundling, A., Burrack, L.S., Bouwer, H.G., and Higgins, D.E. (2004) *Listeria monocytogenes* regulates flagellar motility gene expression through MogR, a transcriptional repressor required for virulence. *Proc Natl Acad Sci USA* **101:** 12318–12323.

Henry, R., Shaughnessy, L., Loessner, M.J., Alberti-Segui, C., Higgins, D.E., and Swanson, J.A. (2006) Cytolysin-dependent delay of vacuole maturation in macrophages infected with *Listeria monocytogenes*. *Cell Microbiol* **8:** 107–119.

Knodler, L.A., Finlay, B.B., and Steele-Mortimer, O. (2005) The *Salmonella* effector protein SopB protects epithelial cells from apoptosis by sustained activation of Akt. *J Biol Chem* **280:** 9058–9064.

Kobayashi, T., Stang, E., Fang, K.S., de Moerloose, P., Parton, R.G., and Gruenberg, J. (1998) A lipid associated with the antiphospholipid syndrome regulates endosome structure and function. *Nature* **392:** 193–197.

Kuijl, C., Savage, N.D., Marsman, M., Tuin, A.W., Janssen, L., Egan, D.A., *et al.* (2007) Intracellular bacterial growth is controlled by a kinase network around PKB/AKT1. *Nature* **450:** 725–730.

Li, M.Z., and Elledge, S.J. (2005) MAGIC, an *in vivo* genetic method for the rapid construction of recombinant DNA molecules. *Nat Genet* **37:** 311–319.

Marquis, H., and Hager, E.J. (2000) pH-regulated activation and release of a bacteria-associated phospholipase C during intracellular infection by *Listeria monocytogenes*. *Mol Microbiol* **35:** 289–298.

Marquis, H., Doshi, V., and Portnoy, D.A. (1995) The broad-range phospholipase C and a metalloprotease mediate listeriolysin O-independent escape of *Listeria monocytogenes* from a primary vacuole in human epithelial cells. *Infect Immun* **63:** 4531–4534.

Molmeret, M., Zink, S.D., Han, L., Abu-Zant, A., Asari, R., Bitar, D.M., and Abu Kwaik, Y. (2004) Activation of caspase-3 by the Dot/Icm virulence system is essential for arrested biogenesis of the *Legionella*-containing phagosome. *Cell Microbiol* **6:** 33–48.

Montes, L.R., Goni, F.M., Johnston, N.C., Goldfine, H., and Alonso, A. (2004) Membrane fusion induced by the catalytic activity of a phospholipase C/sphingomyelinase

from *Listeria monocytogenes*. *Biochemistry* **43:** 3688–3695.
Ohya, K., Handa, Y., Ogawa, M., Suzuki, M., and Sasakawa, C. (2005) IpgB1 is a novel *Shigella* effector protein involved in bacterial invasion of host cells. Its activity to promote membrane ruffling via Rac1 and Cdc42 activation. *J Biol Chem* **280:** 24022–24034.
Pagano, A., Crottet, P., Prescianotto-Baschong, C., and Spiess, M. (2004) *In vitro* formation of recycling vesicles from endosomes requires adaptor protein-1/clathrin and is regulated by rab4 and the connector rabaptin-5. *Mol Biol Cell* **15:** 4990–5000.
Paschen, A., Dittmar, K.E., Grenningloh, R., Rohde, M., Schadendorf, D., Domann, E., *et al.* (2000) Human dendritic cells infected by *Listeria monocytogenes*: induction of maturation, requirements for phagolysosomal escape and antigen presentation capacity. *Eur J Immunol* **30:** 3447–3456.
Philips, J.A., Rubin, E.J., and Perrimon, N. (2005) *Drosophila* RNAi screen reveals CD36 family member required for mycobacterial infection. *Science* **309:** 1251–1253.
Philips, J.A., Porto, M.C., Wang, H., Rubin, E.J., and Perrimon, N. (2008) ESCRT factors restrict mycobacterial growth. *Proc Natl Acad Sci USA* **105:** 3070–3075.
Piper, R.C., and Katzmann, D.J. (2007) Biogenesis and function of multivesicular bodies. *Annu Rev Cell Dev Biol* **23:** 519–547.
Portnoy, D.A., Jacks, P.S., and Hinrichs, D.J. (1988) Role of hemolysin for the intracellular growth of *Listeria monocytogenes*. *J Exp Med* **167:** 1459–1471.
Shaughnessy, L.M., Hoppe, A.D., Christensen, K.A., and Swanson, J.A. (2006) Membrane perforations inhibit lysosome fusion by altering pH and calcium in *Listeria monocytogenes* vacuoles. *Cell Microbiol* **8:** 781–792.
Shen, A., and Higgins, D.E. (2005) The 5′ untranslated region-mediated enhancement of intracellular listeriolysin O production is required for *Listeria monocytogenes* pathogenicity. *Mol Microbiol* **57:** 1460–1473.
Silva, J.M., Li, M.Z., Chang, K., Ge, W., Golding, M.C., Rickles, R.J., *et al.* (2005) Second-generation shRNA libraries covering the mouse and human genomes. *Nat Genet* **37:** 1281–1288.
Smith, A.C., Cirulis, J.T., Casanova, J.E., Scidmore, M.A., and Brumell, J.H. (2005) Interaction of the *Salmonella*-containing vacuole with the endocytic recycling system. *J Biol Chem* **280:** 24634–24641.
Smith, G.A., Marquis, H., Jones, S., Johnston, N.C., Portnoy, D.A., and Goldfine, H. (1995) The two distinct phospholipases C of *Listeria monocytogenes* have overlapping roles in escape from a vacuole and cell-to-cell spread. *Infect Immun* **63:** 4231–4237.
Stuart, L.M., Boulais, J., Charriere, G.M., Hennessy, E.J., Brunet, S., Jutras, I., *et al.* (2007) A systems biology analysis of the *Drosophila* phagosome. *Nature* **445:** 95–101.
Tilney, L.G., and Portnoy, D.A. (1989) Actin filaments and the growth, movement, and spread of the intracellular bacterial parasite, *Listeria monocytogenes*. *J Cell Biol* **109:** 1597–1608.
Wang, S., and Hsu, S.C. (2006) The molecular mechanisms of the mammalian exocyst complex in exocytosis. *Biochem Soc Trans* **34:** 687–690.
Yeung, T., and Grinstein, S. (2007) Lipid signalling and the modulation of surface charge during phagocytosis. *Immunol Rev* **219:** 17–36.

Supporting information

Additional Supporting Information may be found in the online version of this article:

Fig. S1. Association of LBPA with ΔLLO *L. monocytogenes*.
A. Quantification of percentage of LBPA-positive bacteria. HEK-293 cells were treated with FuGene 6 or transfected for 48 h with RABEP1-1 shRNA using FuGene 6, then transferred to collagen-treated 18 mm coverslips in 6-well dishes for 16–18 h. The transfected cells were then infected with ΔLLO *L. monocytogenes* at an moi = 50. For infections of 60 min or less, cells were washed extensively at the indicated time points and cells were fixed with paraformaldehyde. For the 120 min time point, cells were washed extensively with PBS 60 min post infection and gentamicin was added to kill extracellular bacteria. At 120 min post infection, cells were fixed in paraformaldehyde. Cells from all time points were fixed for 16–18 h and stained for immunofluorescence. Remaining extracellular bacteria were stained with an anti-*L. monocytogenes* antibody and AlexaFluor350-conjugated secondary antibody prior to cell permeabilization. Following extensive washing, the cells were permeabilized with saponin buffer and stained for intracellular *L. monocytogenes* and LBPA simultaneously. All bacteria were stained with anti-*L. monocytogenes* antibody and FITC-conjugated secondary antibody. Immunofluorescence staining of LBPA was done with an anti-LBPA primary antibody and Rhodamine Red X-conjugated secondary antibody. Cells were imaged at 1000× total magnification in z-stacks with 0.25 μm z-distance steps. All intracellular bacteria were analysed from at least 20 host cells at each time point in four independent experiments. Results shown are the means ± SEM of all experiments. No statistical difference between the conditions was observed.
B. Representative images taken at various time points of bacteria identified as LBPA-positive (right) or LBPA-negative (left). Arrows indicate association of LBPA staining with *L. monocytogenes*.
Fig. S2. Knockdown of RAB5C, CTSL1 or SEC15L1 in HEK-293 cells does not cause increased uptake of ΔLLO *L. monocytogenes*. 1.0×10^4 HEK-293 cells per well were seeded in a black, clear-bottom 96-well plate. Approximately 24 h later, cells were treated with FuGene 6 or transfected with shRNAs targeting (A) endosomal pathway components RAB5C (early endosome) and CTSL1 (lysosome) or (B) exocyst pathway component SEC15L1 using FuGene 6. Sixty hours after transfection, cells were infected with ΔLLO *L. monocytogenes* at an moi = 5. Gentamicin was added 1 h post infection to kill extracellular bacteria. At 2 h post infection, host cells in three wells per condition were lysed. Appropriate dilutions of the lysates were plated on LB plates and intracellular bacteria were enumerated by counting the number of colony-forming units. Results shown are the means ± standard deviation of one of three experiments with similar results.
Table S1. shRNAs in the vesicular trafficking library. shRNAs were selected from a previously constructed genome-wide pSMC2 shRNA library. In total, 211 shRNAs targeting gene products with functions related to vesicular trafficking were included

in the screening library. The gene function information is based upon the NCBI Gene database (http://www.ncbi.nlm.nih.gov). Hairpin sequences can be found using the hairpin ID number at http://codex.cshl.edu.